Two-carrier transport and ferromagnetism in FeSe thin films

X. J. Wu, Z. Z. Zhang, J. Y. Zhang, B. H. Li, Z. G. Ju et al.

Related Articles

Crossover to striped magnetic domains in Fe1−xGax magnetostrictive thin films
Appl. Phys. Lett. 101, 092404 (2012)

Luminescence-based magnetic imaging with scanning x-ray transmission microscopy
Appl. Phys. Lett. 101, 083114 (2012)

Strain induced magnetic domain evolution and spin reorientation transition in epitaxial manganite films
Appl. Phys. Lett. 101, 022411 (2012)

Influence of the winding number on field- and current driven dynamics of magnetic vortices and antivortices
J. Appl. Phys. 112, 013917 (2012)

Current-induced motion of a transverse magnetic domain wall in the presence of spin Hall effect
Appl. Phys. Lett. 101, 022405 (2012)
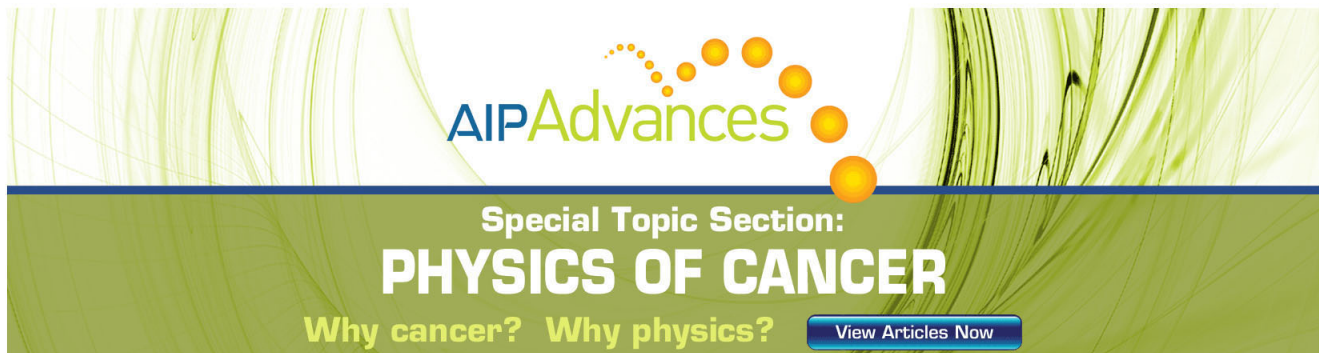
Additional information on J. Appl. Phys.

Journal Homepage: http://jap.aip.org/

Journal Information: http://jap.aip.org/about/about_the_journal

Top downloads: http://jap.aip.org/features/most_downloaded

Information for Authors: http://jap.aip.org/authors

Two-carrier transport and ferromagnetism in FeSe thin films

X. J. Wu,[1] Z. Z. Zhang,[2] J. Y. Zhang,[2,a)] B. H. Li,[2] Z. G. Ju,[2] Y. M. Lu,[2] B. S. Li,[2] and
D. Z. Shen[2]

[1]*Key Laboratory of Excited State Processes, Changchun Institute of Optics, Fine Mechanics and Physics,
Chinese Academy of Sciences, Changchun 130033, People's Republic of China and Graduate School
of the Chinese Academy of Sciences, Beijing 100049, People's Republic of China*
[2]*Key Laboratory of Excited State Processes, Changchun Institute of Optics, Fine Mechanics and Physics,
Chinese Academy of Sciences, Changchun 130033, People's Republic of China*

α- and β-FeSe thin films were grown by metal organic chemical vapor deposition. Compared to the other parameters, the growth temperature shows decisive influence on the phase transition of the FeSe samples. In temperature-dependent electrical measurements, n-type to p-type reversion was observed for both the α- or and β-FeSe samples. Furthermore, the p-type character of the films becomes more and more obvious with increasing the Se/Fe atomic ratio in the samples. Ferromagnetism was observed in the α-FeSe films although which is not supported by calculation on density of states. The ferromagnetic character shows significant dependence on Se/Fe atomic ratio in the films and was attributed to the Fe vacancies or Fe clusters in the α-FeSe thin films. The magnetic domain and hysteresis loop of the β-FeSe thin films are also studied. © *2008 American Institute of Physics*. [DOI: 10.1063/1.2936977]

I. INTRODUCTION

FeSe is one of the promising candidates for spin injection in GaAs—or ZnSe-based spin electronic devices due to the ferromagnetism and the matched lattice.[1] However, the properties of FeSe thin films strongly depend on the fabricating parameters, which affects the applications of FeSe materials. For example, FeSe grown at different conditions exhibits the tetragonal α-FeSe phase (isotypic with anti-PbO structure) or the hexagonal β-FeSe phase (isotypic with NiAs structure).[2–4] It was accepted that β-FeSe has the ferromagnetism nature.[5] Oppositely, for α-FeSe, there still exists confusions on the magnetic properties.[5,6] In previous work, we mentioned that the α-FeSe films show significant change in electrical and magnetic properties which depended on various growth parameters.[6] For either understanding the mechanism of FeSe ferromagnetism or fabricating the FeSe-based spin electronic devices, it is necessary to clarify the growth parameter influences on FeSe properties.

In present work, it was found that the growth parameters, especially temperature, show effects on the phase structure and Se/Fe atomic ratio of FeSe. The electrical properties were mainly dependent on Se/Fe atomic ratio of the samples. Correspondingly, the magnetic properties of the samples were found to be dependent on both the phase structure and the Se/Fe ratio. Furthermore, the ferromagnetism origin of the α-FeSe thin films was also clarified.

II. EXPERIMENTAL PROCEDURE

Iron selenide thin films were grown by low-pressure metal organic chemical vapor deposition (LP-MOCVD) with a chamber pressure fixed at about 1.0×10^4 Pa. To measure the electrical properties of the samples conveniently, c-plane sapphire, which is insulating, was used as the substrate. H_2Se and iron pentacarbonyl [$Fe(CO)_5$] were used as precursors, where the flow rates of which [1.6×10^{-5}–1.3×10^{-4} mol/min for H_2Se and 3.4×10^{-6} mol/min for $Fe(CO)_5$] were controlled by respective mass-flow controllers. High purity hydrogen (99.999%) was used as carrier gas with total flow rate of 1.9 l/min. The growth temperatures were 350–500 °C.

A rotating anode x-ray diffractometer with Cu $K\alpha$ radiation of 0.154 nm was employed to characterize the structure of the FeSe thin films. The morphology of the samples was studied by scanning electron microscopy (SEM) and atomic force microscopy (AFM). The Se/Fe atomic ratios in the films were measured by energy dispersive spectroscopy (EDS) on a Hitachi S4800 scanning electron microscope. A Lake Shore 7707 Hall measurement system was employed to characterize the electrical properties of the thin films. The magnetic properties of the FeSe films were studied by a vibrating sample magnetometer (VSM), a magnetic force microscope (MFM), and first-principle calculation for the density of states (DOS).

III. RESULTS AND DISCUSSIONS

Figure 1(a) is the x-ray diffraction (XRD) patterns of the samples grown at 350 °C with different $H_2Se/Fe(CO)_5$ molar flow ratios. The peak at 41.68° is from the sapphire substrate. For the samples grown with flow ratios of 37, 13, and 6.1, three diffraction peaks located at 32.3°, 49.5°, and 67.9° can be observed in the patterns, which are assigned to the (002), (003), and (004) diffractions of α-FeSe, respectively.[7] The pure (00l) orientation indicates that the α-FeSe films have acceptable crystal quality. When the flow ratio was decreased further to 4.6, an intense Fe (110) diffraction peak appears because the atmosphere has changed into Fe-rich

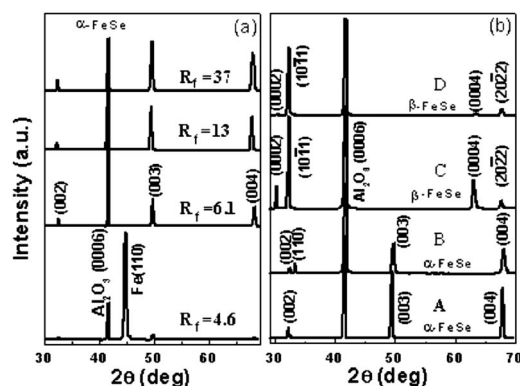a)Author to whom correspondence should be addressed. Electronic mail: zhangjy53@yahoo.com.cn.

FIG. 1. (a) X-ray diffraction patterns of the FeSe thin films grown at 350 °C with different $H_2Se/Fe(CO)_5$ flow ratios and (b) x-ray diffraction patterns of the FeSe thin films prepared at 350, 400, 450, and 500 °C, which were labeled as samples A, B, C, and D, respectively.

environment. Fortunately, the FeSe films still maintains the tetragonal structure with good (001) orientation. In previous work, we mentioned that the α-FeSe film has (001) orientation growth characteristic on different substrates. In this contribution, (001) orientation growth with varying $H_2Se/Fe(CO)_5$ flow ratio in wide range proved this nature again.

Figure 1(b) shows the XRD patterns of the FeSe films grown at 350, 400, 450, and 500 °C, which were labeled as samples A, B, C, and D, respectively. $H_2Se/Fe(CO)_5$ flow ratio of 13 was used here because the atomic Se/Fe ratio in the film can approach 1:1. With increasing the growth temperature from 350 to 400 °C, the film degraded from (001) to mixed orientation. A (110) peak appears at the large-angle-side of the (002) peak. When the temperature was increased to 450 °C, the film transited from α- to β-phases. The β-(0001) and β-(10$\bar{1}$1) peaks can be observed clearly. The α-(001) peaks, especially the intense (003) peak, disappear from the XRD patterns. Sample D, which is grown at 500 °C, shows the same structural characteristic with sample C. Obviously, compared to flow ratio, the growth temperature shows pivotal influence on the phase reversion of FeSe.

Besides in XRD patterns, the phase reversion also shows clear marks in morphology observation. Figure 2 shows surface morphology SEM images of samples A–D. The samples grown at various temperatures show widely different morphologies. For sample A, which was grown at 350 °C, the surface looks fairly plane and smooth. When the temperature was increased to 400 °C, lots of grains were generated on the surface, as sample B looks. It is in accordance with the mix-oriented XRD pattern in Fig. 1(b). For the growth at
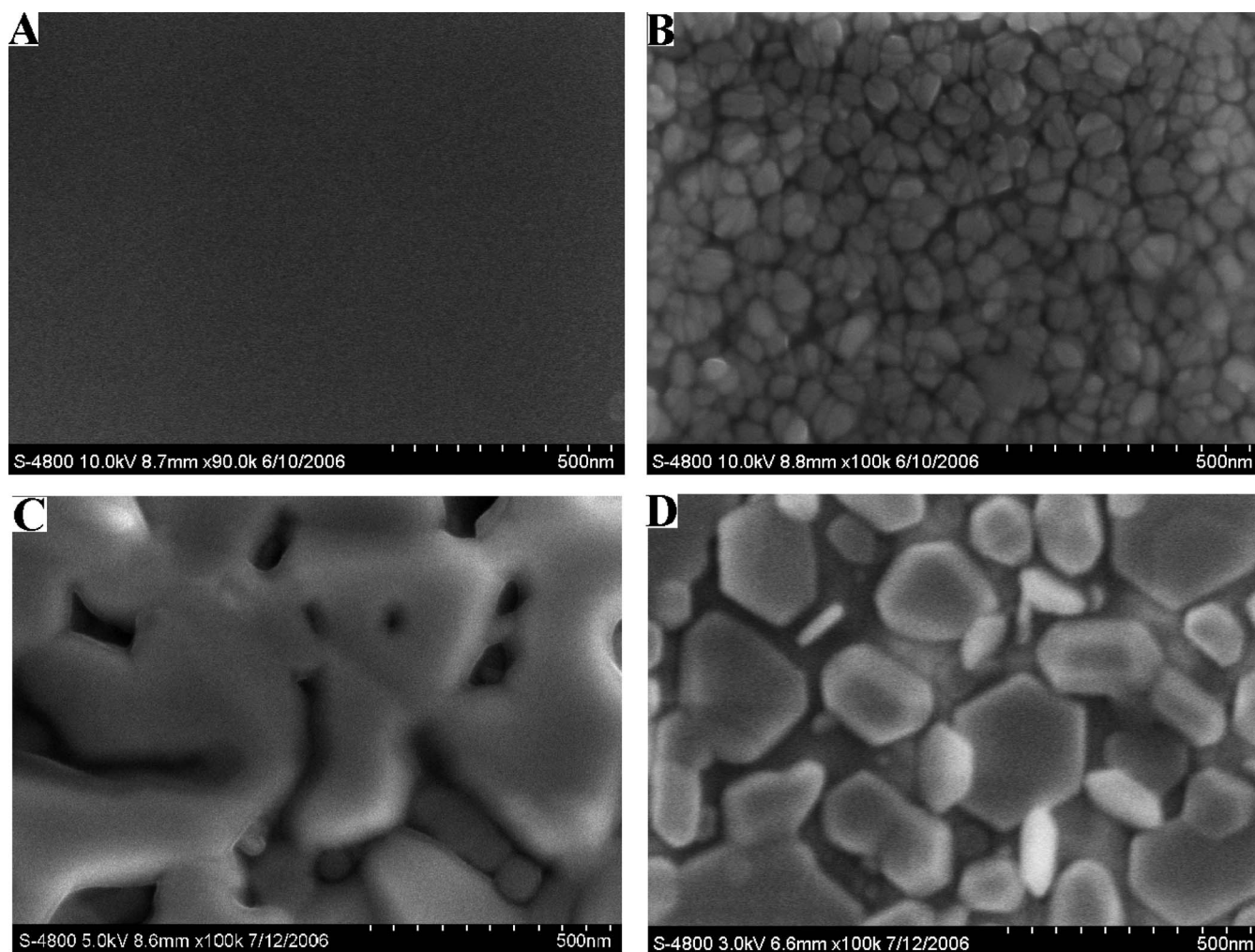

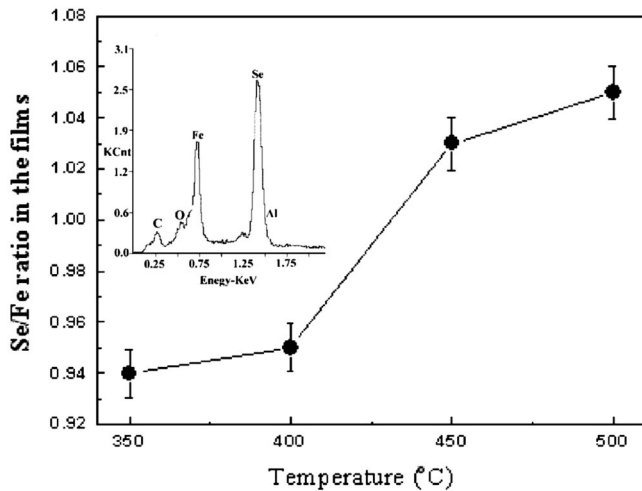FIG. 2. The SEM images of samples A–D.

FIG. 3. The atomic ratio of Se/Fe in samples A–D. The inset is a typical EDS pattern of the samples.

450 °C, the surface evolved into connected islands. The size of the islands is much larger than the grains on sample B. It should be noted that the islands exhibit some hexagonal characteristic, which also means that the film has reversed from α- to β-phases. With increasing the temperature to 500 °C, the surface islands changed into isolated islands and the hexagonal characteristic looks more obvious.

In general, varying the flow ratio of precursors is used to change the atomic ratio in materials. Here, varying growth temperature also changes the Se/Fe atomic ratios of FeSe films with keeping precursors flow ratio constant. The Se/Fe atomic ratios of samples A–D are shown in Fig. 3, which were measured by EDS. Although the atomic Se/Fe ratio in the films approaches to 1:1, it shows a small increasing tendency with increasing growth temperature. This is because high temperature accelerates the pyrolyzing of H_2Se [$Fe(CO)_5$ can be pyrolyzed completely as the temperature reaches 179 °C]. The inset shows a typical EDS pattern of the samples, where the aluminum, oxygen, and carbon signals are from the sapphire substrate and the absorbed CO_2, respectively.

It usually makes us believe that the change in structure would bring effects on electrical properties. Based on this intention, Hall measurements were performed in the Van der Pauw configuration. Because the ferromagnetism of samples may disturb the Hall results, the measurements were performed under magnetic fields up to 0.9 T.[7] Table I lists the conduction type of samples A, B, and C at the temperature range of 85–360 K. The result for sample D was not adopted

because the resistance of sample D is so large that the HMR7707 system showed "current leak" warning during the measurements. The label $p(n)$ denotes that p-type results dominate the numerous repeated measurements, vice versa. For all the three samples, n- to p-type reversion was observed. The conduction reversion indicates that both α- and β-FeSe show two-carrier transport characteristic. Especially for α-FeSe, the conductivity reversion from n- to p-type with increasing temperatures has been attributed to the thermal activation of localized holes in the thin films, which was supported by both Hall measurements and calculation on energy bands in our previous work.[8] As shown in Table I, sample A exhibits n-type conduction in the low temperature region and begins to show p-type characteristic from 180 K, and finally converts to p-type fully after 240 K. For sample B, the n-p reversion comes earlier than sample A during the temperature increase. For sample C, the n-p reversion took place almost at the very start of temperature increase. In other words, the higher the growth temperature is, the stronger the p-type characteristic seems. By all appearances, the strengthening of p-type conduction does not lie on the phase reversion, because the difference in electrical properties also exists between the samples with the same structure (samples A and B). Therefore, the increase of Se/Fe ratio is a more acceptable factor for the changing of conduction because Fe vacancies in FeSe films can act as acceptors. Higher acceptor concentration can ionize more holes at a certain temperature, which brings n-p reversion earlier.

Since the conduction can be changed by the thermal ionization mentioned above, it would also be influenced by light illumination. The temperature dependent resistances of samples A–D measured under natural room light illumination and in dark are shown in Figs. 4(a)–4(d), respectively. From the different evolvements of the resistance, it could be found that both thermal excitation and light excitation have significant influence on the sample resistance. In Fig. 4(a) for sample A, the resistance shows a monotone increase as the temperature rises. It results from that the n-type conduction of sample A was compensated gradually by holes activated by thermal energy. In the case of light irradiation, the resistances are higher than that measured in the dark. It indicates that light excitation works, even more efficiently than thermal activation does. In Fig. 4(b), because sample B shows a stronger p-type characteristic than sample A, the activated holes decrease the resistance of the FeSe film. In Figs. 4(c) and 4(d) for samples C and D, the activated holes also show significant effect on the resistance. Based on the Hall results and resistance evolvements, hole ionization should be the

TABLE I. The temperature dependence of conduction type of samples A, B, and C. It was measured by a 7707 Hall measurement system (from Lake Shore) in the Van der Pauw configuration. The magnetic field was set at 0.9 T.

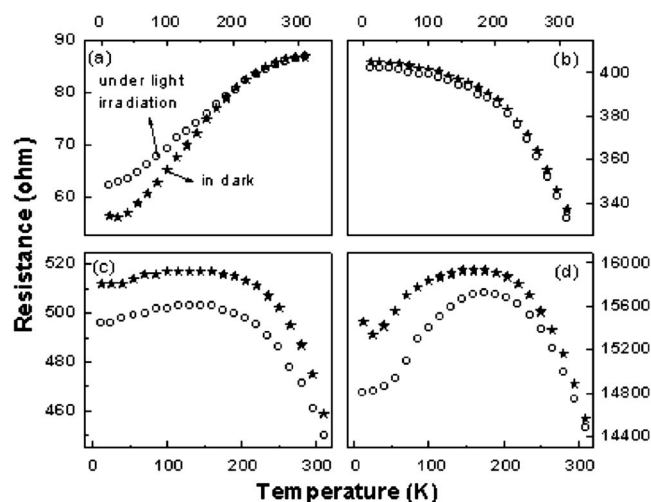| Sample	Temperature (K)										
	85	100	120	140	160	180	200	240	280	300	360
A (350 °C)	$n(p)$	$n(p)$	$n(p)$	$n(p)$	$n(p)$	$p(n)$	$p(n)$	p	p	p	p
B (400 °C)	$n(p)$	$n(p)$	$p(n)$	$p(n)$	$p(n)$	p	p	p	p	p	p
C (450 °C)	$p(n)$	p	p	p	p	p	p	p	p	p	p

FIG. 4. [(a)–(d)] The temperature dependent resistivity of samples A–D. The black star and the hollow circle denote the experiment points under natural illumination and in dark, respectively.

FIG. 6. (Color online) The calculated density of states (up- and down-spin) of α- and β-FeSe. The Fermi energy is defined to be at zero. (a) and (b) are the results for α- and β-FeSe, respectively.

dominant reason for the n-p reversion in both the α- and β-FeSe samples. Note that the resistances under light illumination and in dark tend to coincide with each other with increasing temperature. This is because almost all the localized holes were thermal ionized in the high temperature region. The resistance of samples A–D shows a significant increase with increasing growth temperature. It is caused by the more and more aggravating cranny on the samples, as shown in Fig. 2.

In previous work,[6] we found that the magnetic properties of the FeSe thin films vary in a wide range with changing growth parameters. Energy band calculation on perfect FeSe is helpful for studying the influences of growth parameters on the properties of FeSe thin films. The density-functional theory within local spin density approximation was used here. The unit cells of the α- and β-FeSe are sketched in Fig. 5. As seen, there are significant differences in coordination number and arrangement of atoms between the two structures. It is believed to bring wide differences in the energy band structure. The lattice constants of the α- and β-FeSe obtained from XRD were adopted as the input parameters for the theoretical modeling. Figures 6(a) and 6(b) depict the calculated spin-polarized DOS of α- and β-FeSe, respectively. The Fermi energy is defined to be at zero. For perfect
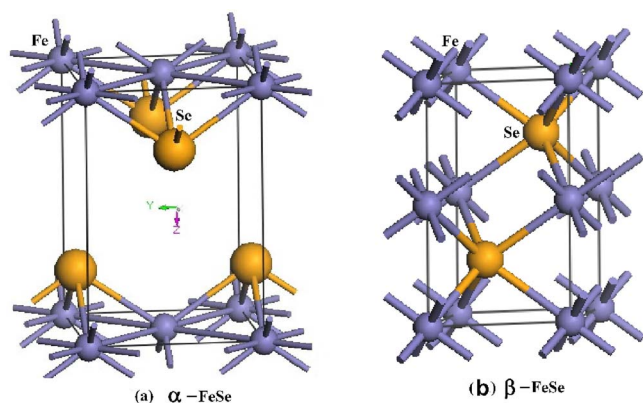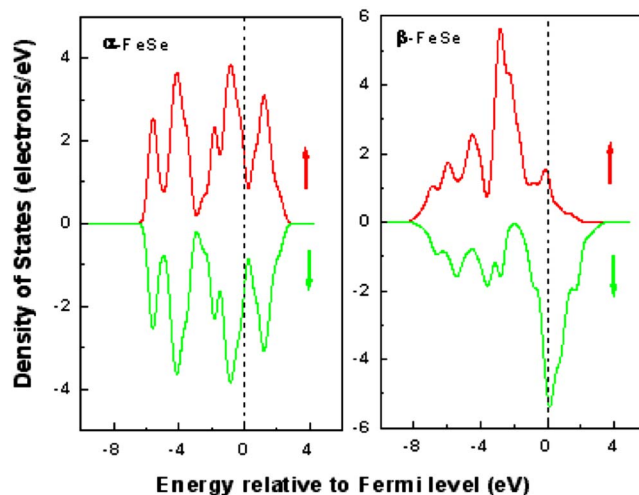
α-FeSe crystal, the DOS for up- and down-spin bands show a precise symmetry distribution VS energy. Near the Fermi level, the DOSs for the up- and down-spin electrons possess considerable values, and the total magnetic moment is equal to zero. Therefore, perfect, stoichiometric α-FeSe is a nonferromagnetic metal. In contrast, the DOSs of β-FeSe for up- and down-spin bands show significant difference near the Fermi level. It indicates that β-FeSe is a natural ferromagnetic material. Note that the DOSs for both majority and minority spin bands show nonzero values near the Fermi level, that is, to say, β-FeSe also has metal characteristic.

As the calculation pointed out, stoichiometric α-FeSe was also found experimentally to show nonferromagnetism. However, nonstoichiometric α-FeSe samples show distinct ferromagnetism, whose hysteresis loop shapes are intensively dependent on the growth parameters. Obviously, the ferromagnetism originates from the imperfection of α-FeSe films. Figure 7 shows the hysteresis loops of another series of α-FeSe films with various Se/Fe atomic ratios under in-
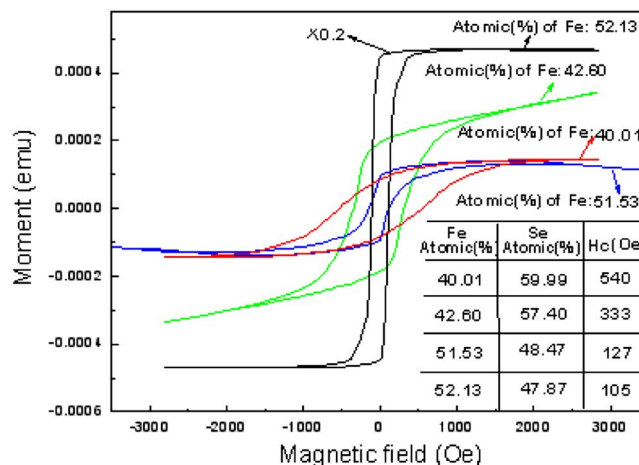

FIG. 7. (Color online) Hysteresis loops of α-FeSe films with various Se/Fe ratios at room temperature. The magnetic field is parallel to the sample surface. The inset lists the atomic ratio of Fe/Se and coercive forces of the FeSe thin films.
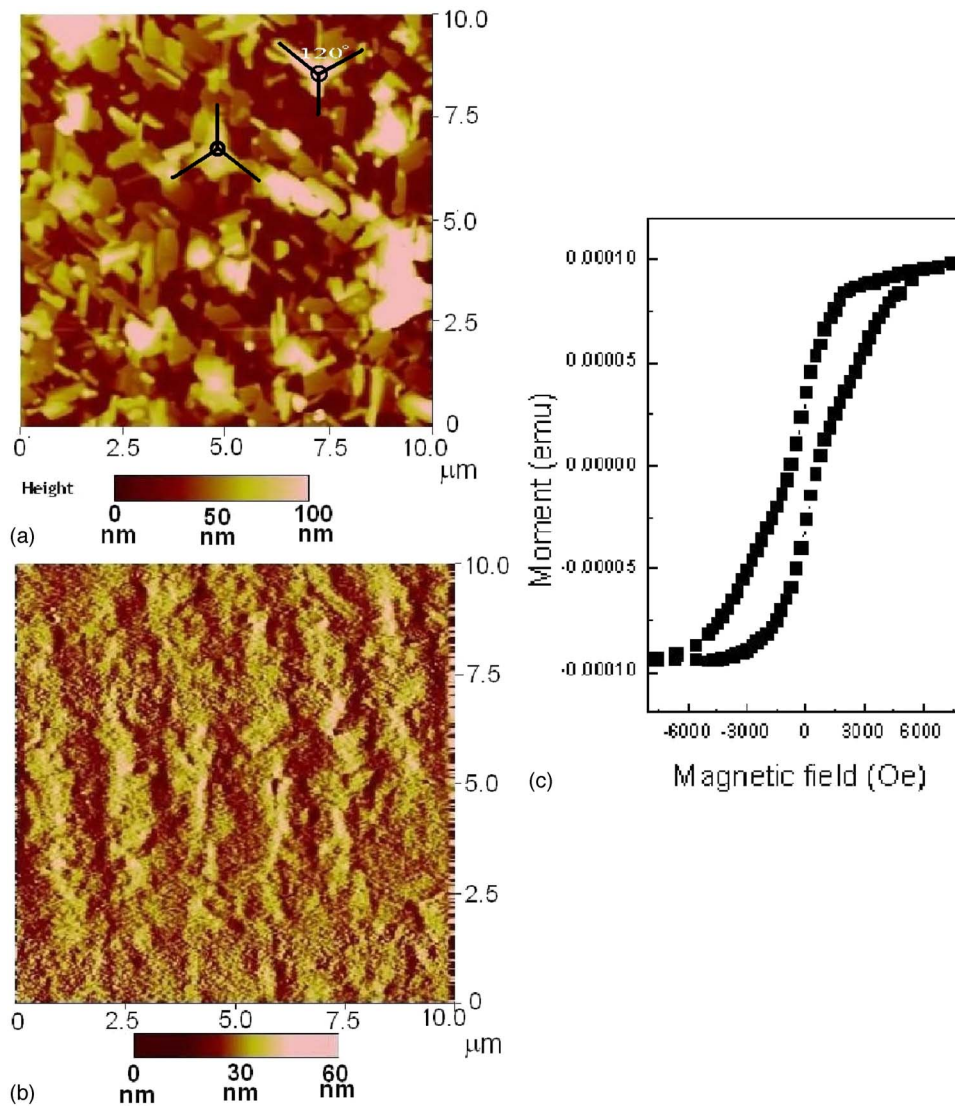

FIG. 5. (Color online) Unit cells used in this paper for α- and β-FeSe

FIG. 8. (Color online) (a) AFM images and (b) MFM images of sample C at room temperature. The images are 10×10 μm^2. The scanning height of MFM image is 100 nm. (c) The room temperature hysteresis loops of sample C under in-plane magnetic field.

plane magnetic fields. The inset lists the atomic ratio of Se/Fe and coercive force of the samples. It is observed that all the ferromagnetic α-FeSe thin films have Se/Fe ratio with a certain deviation from 1:1. The coercive forces are about 540, 333, 127, and 105 Oe for the samples with Fe contents of 40.01, 42.60, 51.53, and 52.13 at. %, respectively. It is found that the coercive forces of the Se-rich samples are significantly larger than that of Fe-rich samples. The ferromagnetism with larger coercive forces observed in Se-rich samples are attributed to the Fe vacancies, where the mechanism is similar to the case of Fe_7S_8 pyrrhotite.[9] For the Fe-rich samples, the hysteresis loops show isotropy under different magnetic field directions (not shown here), which is different from most cases of oriented thin films. Considering the small coercive forces, the ferromagnetism of Fe-rich samples should come from large numbers of Fe clusters in the films. As shown in Fig. 7, all the samples show single-coercive-force characteristic. The "large" and "small" coercive forces were never observed simultaneously in one sample in our experiments. It is in accordance with the fact that the Fe vacancy and Fe cluster are difficult to coexist in one FeSe sample.

For the β-FeSe thin films, the ferromagnetism was observed experimentally as expected. AFM and MFM images and *M-H* curve at room temperature are shown in Fig. 8 to characterize the thin films. Figure 8(a) is the two-dimensional AFM topography images of sample C, which are 10×10 μm^2 scans. A configuration with hexagonal structure was observed, as marked in the image. Figure 8(b) is the room temperature MFM image of sample C after subtracting the AFM background. The stripe domains could be observed clearly in β-FeSe, which usually appears in most ferromagnetic films. The *M-H* curve of sample C is also shown here as Fig. 8(c). It exhibits a hysteresis loop different from common loops, which is obviously a superposition of two loops with different coercive forces. In the XRD pattern of sample C, it is shown that the film includes $(10\bar{1}1)$ orientation besides (0001) orientation. Taking account of the magnetocrystalline anisotropy of FeSe film, it is not difficult to understand the loop shape in Fig. 8(c).

IV. CONCLUSIONS

In summary, the structure, two-carrier transport and ferromagnetism of FeSe thin films with anti-PbO and NiAs structures were studied. The growth temperature is an impor-

tant factor for the structure transition between α- and β-phases. Growth temperature higher than 450 °C benefits the forming of β-phase. The Se/Fe atomic ratio affects the electrical and magnetic properties of the films. As the Se/Fe atomic ratio rises, the p-type conduction dominates the carrier transport of the samples gradually. It was attributed to the increase of acceptorlike Fe vacancies in the FeSe films. In accordance with the first principle calculation on DOS, the stoichiometric α-FeSe thin films are nonferromagnetic. However, nonstoichiometric α-FeSe thin films show ferromagnetism, which were attributed to the Fe vacancy and Fe clusters for the cases of Se-rich and Fe-rich films, respectively.

ACKNOWLEDGMENTS

[1] Y. Takemura, H. Suto, N. Honda, K. Kakuno, and K. Saito, J. Appl. Phys. **81**, 5177 (1997).

[2] A. R. Lennie, K. E. R. England, and D. J. Vaughan, Am. Mineral. **80**, 960 (1995).

[3] H. Tokutaro, M. Seijiro, and T. Noboru, J. Phys. Soc. Jpn. **9**, 496 (1954).

[4] C. E. M. Camposa, J. C. de Limaa, T. A. Grandia, K. D. Machadoa, and P. S. Pizani, Solid State Commun. **123**, 179 (2002).

[5] H. Tokutaro and C. Shu, J. Phys. Soc. Jpn. **11**, 666 (1956).

[6] Q. J. Feng, D. Z. Shen, J. Y. Zhang, B. S. Li, B. H. Li, Y. M. Lu, X. W. Fan, and H. W. Liang, Appl. Phys. Lett. **88**, 012505 (2006).

[7] X. J. Wu, Z. Z. Zhang, J. Y. Zhang, Z. G. Ju, D. Z. Shen, B. H. Li, C. X. San, and Y. M. Lu, J. Cryst. Growth **300**, 483 (2007).

[8] X. J. Wu, D. Z. Shen, Z. Z. Zhang, J. Y. Zhang, K. W. Liu, B. H. Li, Y. M. Lu, B. Yao, D. X. Zhao, B. S. Li, C. X. Shan, X. W. Fan, H. J. Liu, and C. L. Yang, Appl. Phys. Lett. **90**, 112105 (2007).

[9] A. Okazaki, J. Phys. Soc. Jpn. **16**, 1162 (1961).